

# Copper complexes bearing 2-aminobenzothiazole derivatives as potential antioxidant: Synthesis, characterization

J. Joseph <sup>\*</sup>, G. Boomadevi Janaki

Department of Chemistry, Noorul Islam Centre for Higher Education, Kumaracoil-629 180, Tamil Nadu, India

## ARTICLE INFO

### Article history:

Received 14 April 2016

Accepted 17 June 2016

Available online xxxx

### Keywords:

Acetoacetanilide

Knoevenagel

Antioxidant

Screening

## ABSTRACT

Novel copper complexes of Schiff base ligands of 2-aminobenzothiazole derivatives were synthesized by the condensation of Knoevenagel condensate of acetoacetanilide (obtained from substituted benzaldehydes and acetoacetanilide) and 2-aminobenzothiazole. They were characterized by elemental analysis, IR, <sup>1</sup>H NMR, UV–Vis., molar conductance, magnetic susceptibility measurements and electrochemical studies. Based on the magnetic moment and electronic spectral data, square planar geometry has been suggested for all the complexes. Antibacterial and antifungal screening of the ligands and their complexes reveal that all the complexes show higher activities than the ligands. The binding behaviour of the complexes with calf thymus DNA has been investigated by electronic absorption spectra, viscosity measurements and cyclic voltammetry. The DNA binding constants reveal that all these complexes interact with DNA through intercalation binding mode. Superoxide dismutase and antioxidant activities of the copper complexes have also been studied. The antioxidant activities of the complexes showed higher activities. Thermal denaturation studies suggested the nature binding affinity of copper complexes with CT-DNA. All complexes exhibit suitable Cu(II)/Cu(I) redox potential to act as antioxidant enzymes mimic. Further, the copper complexes also showed catalase activity. It is hoped that copper complexes were capable of decrease ROS levels or reduce oxidative stress in Alzheimer's patients.

© 2016 Elsevier B.V. All rights reserved.

## 1. Introduction

A natural products of  $\beta$ -diketones of siphonarienedione and cyclopitalantin possessing medicinal activity as well as  $\beta$ -diketones are used as a powerful intermediates for the organic synthesis. 1,3-diketone system of the polyphenol diferuloylmethane (curcumin) exhibits a variety of pharmacological activities including antiinflammatory, anticarcinogenic, antibacterial and antifungal activities, hepato- and nephro-protective [1–2], thrombosis suppressing [3], myocardial infarction protective [4] most of which are accredited to its antioxidant and radical scavenging properties. Curcumin based analogs of difluoro Knoevenagel condensate and their Schiff base copper complexes exhibited more effective in protease inhibition and apoptosis inducers in cancer cells [5] (Scheme 1).

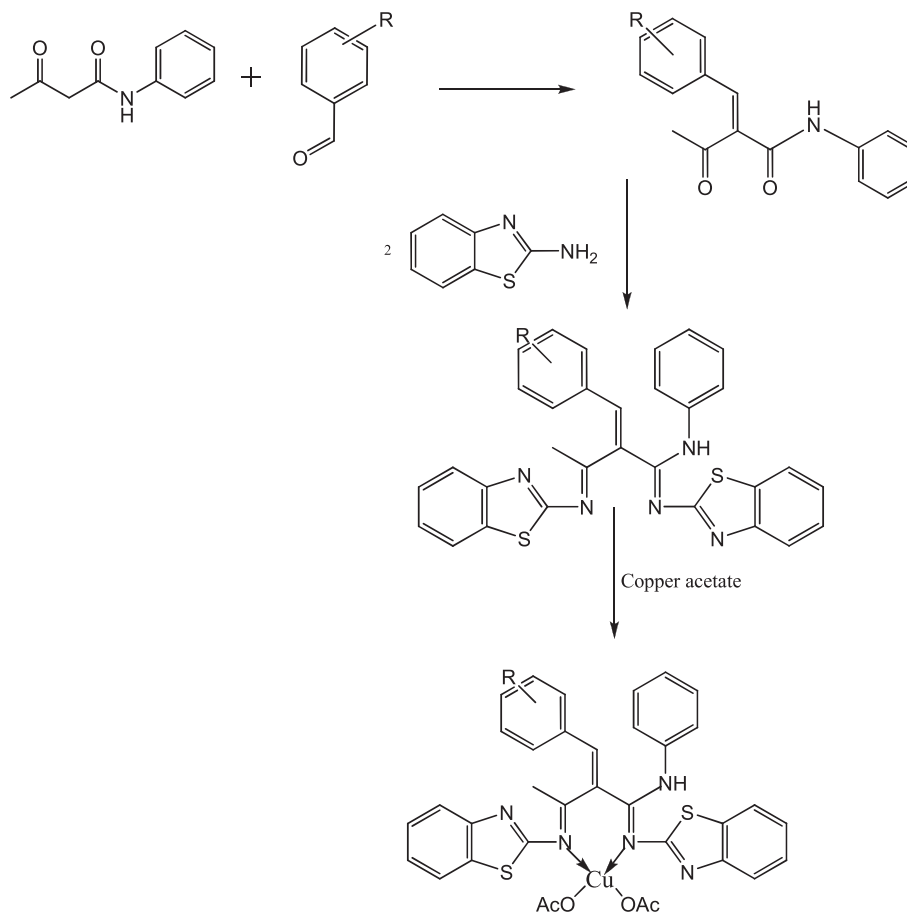
Schiff bases and their complexes have been studied for their variety of biological actions by virtue of the azomethine linkage, due to its ability to reversibly bind oxygen, catalytic activity in hydrogenation of olefins, transfer of an amino group, photochromic properties and complexing ability towards some toxic metals. This high affinity for chelation of the Schiff bases towards the transition metal ions is utilized in preparing their solid complexes [6–10].

The biological activity greatly depends on the nature of the metal ion and the donor atoms of the ligands [11–12]. Metal complexes of Schiff bases derived from substituted aldehydes and heterocyclic compounds containing nitrogen, sulphur and/or oxygen as ligand atoms are of interest as simple structural models of more complicated biological systems [13–15]. Many of the aldehydes tested were found to have highly potent antimicrobial activity. These aldehydes may act as good candidates for practical applications as well as interesting lead compounds for the development of novel antimicrobial agents. Schiff bases of 2-aminobenzothiazole derivatives have been of great importance due to their synthetic flexibility and biological activity of their metal complexes [16]. Diazotized 2-aminobenzothiazole with 1,3-dicarbonyl compounds (benzoylacetone, methyl acetoacetate and acetoacetanilide) obtained a new series of tridentate compounds exist in the intramolecularly hydrogen bonded azo-enol tautomeric form in which one of the carbonyl groups of the dicarbonyl moiety had enolised and hydrogen bonded to one of the azo nitrogen atoms. The stable complexes showed a normal paramagnetic moment [17].

The interaction of transition metal complexes with nucleic acids is a major area of research due to the utility of these complexes in the design and development of synthetic restriction enzymes, spectroscopic probes, site specific cleavers and molecular photoswitches [18]. The transition metal complexes are currently used as artificial nucleases are because of their diverse structural feature, and the possibility to tune their redox potential through the choice of proper ligands [19].

<sup>\*</sup> Corresponding author.

E-mail address: [chem\\_joseph@yahoo.co.in](mailto:chem_joseph@yahoo.co.in) (J. Joseph).



**Scheme 1.** Schematic outline of synthesis of ligands and their complexes.

Copper(II) complex is probably the most extensively studied among the transition metal ions. This is due to their lability, their high affinity with different ligands and the wide variety of ligands geometries that can accommodate significant role either in naturally occurring biological systems or as pharmacological agents like (CuZn-SOD) superoxide dismutase and its disproportionate the toxic  $O_2^-$  radical into molecular oxygen and hydrogen peroxide [20–22]. In the present study we describe the synthesis and characterization of new series of curcumin analog copper complexes of Knoevenagel condensate of Schiff base of 2-aminobenzothiazole.

## 2. Experimental

### 2.1. Material

All chemicals and solvents were analar grade and were purchased from Merck. All supporting electrolyte solutions were prepared using analytical grade reagents. Calf thymus DNA purchased from Genie Biolab, Bangalore, India.

### 2.2. Instrumentation

The amount of copper present in the copper complexes was estimated using ammonium oxalate method. Elemental analysis of ligands and their copper complexes were carried out using Elementar Vario EL III. Molar conductance of the complexes was measured using a coronation digital conductivity meter. The  $^1H$  NMR spectra of the ligands were recorded using TMS as internal standard. Chemical shifts are expressed in units of parts per million relative to TMS. The IR spectra of the ligands and their copper complexes were recorded on a Perkin-Elmer 783

spectrophotometer in 4000–200  $cm^{-1}$  range using KBr disc. Electronic spectra were recorded in a Systronics 2201 Double beam UV–Vis., spectrophotometer within the range of 200–800 nm regions. Magnetic moments were measured by Guoy method and corrected for diamagnetism of the component using Pascal's constants. Cyclic voltammetry was performed on a CHI 604D electrochemical analyzer with three electrode system of glassy carbon as the working electrode, a platinum wire as auxiliary electrode and Ag/AgCl as the reference electrode. Tetrabutylammoniumperchlorate (TBAP) was used as the supporting electrolyte. Solutions were deoxygenated by eradication with  $N_2$  previous to measurements. The interactions between metal complexes and DNA were studied using electrochemical and electronic absorption techniques.

### 2.3. Preparation

#### 2.3.1. Synthesis of $\beta$ -Ketoanilides

An ethanolic solution of acetoacetanilide (1 M), was added drop wise in the ethanolic solution of substituted benzaldehydes ( $L^1$ -anisaldehyde,  $L^2$ -salicylaldehyde,  $L^3$ -2-bromo benzaldehyde,  $L^4$ -3,4-dimethoxy benzaldehyde) (1 M) in the presence of anhydrous potassium carbonate (1 M) in the mixture with stirring. The resulting mixture was refluxed for about 8 h. The solid thus obtained was filtered, dried and recrystallized from ethanol to obtain yellow colored  $\beta$ -ketoanilide(s).

#### 2.3.2. Synthesis of Schiff Bases

Yellow colored  $\beta$ -ketoanilide(s) (1 M) was dissolved in ethanol added drop wise to 2-aminobenzothiazole (2 M) and stirring at room temperature. The resulting solution was refluxed about 8 h and the

product formed was poured into ice. The solid mass was obtained undergo filtered and dried. Then, it was washed with petroleum ether in order to remove nonpolar impurities. The reaction product was reduced to one third of volume and yield brown colored substance.

### 2.3.3. Synthesis of Complexes

An ethanolic solution of Schiff base (1 M) was mixed with copper acetate (1 M) in ethanol solution with continuous stirring. The mixture was then refluxed for 7 h till the volume of the solution was reduced to 10 mL. The complexes were precipitated in dry diethylether. The solid product obtained was filtered, washed with distilled water and cold ethanol and then dried *in vacuum*.

### 2.4. DNA Binding Studies

The binding interactions between metal complexes and DNA were studied using electrochemical and electronic absorption methods by using different concentrations of CT-DNA. Calf thymus DNA was stored at 4 °C. The DNA stock solutions were prepared with buffer solution (50 mM Tris-HCl at pH 7.2). The stock solutions of the complexes were prepared by dissolving copper complexes in DMSO and diluting with the corresponding buffer to the required concentration for all experiments. This resulted in a series of solutions with varying concentrations of DNA but with a constant concentration of the complex. The absorbance (A) of the most red-shifted band of complex was recorded after each successive additions of CT DNA. The intrinsic binding constant,  $K_b$ , was determined from the plot of  $[DNA] / (\epsilon_a - \epsilon_f)$  vs  $[DNA]$ , where  $[DNA]$  is the concentration of DNA in base pairs,  $\epsilon_a$ , the apparent extinction coefficient which is obtained by calculating  $A_{obs} / [complex]$  and  $\epsilon_f$  corresponds to the extinction coefficient of the complex in its free form. The data were fitted to the following equation where  $\epsilon_b$  refers to the extinction coefficient of the complex in the fully bound form.

$$[DNA]/(\epsilon_a - \epsilon_f) = [DNA]/(\epsilon_b - \epsilon_f) + 1/K_b(\epsilon_b - \epsilon_f) \quad (1)$$

Each set of data, when fitted to the above equation, gave a straight line with a slope of  $1/(\epsilon_b - \epsilon_f)$  and a y-intercept of  $1/K_b(\epsilon_b - \epsilon_f)$ .  $K_b$  was determined from the ratio of the slope to intercept.

### 2.5. Thermal Denaturation

In order to identify the thermal behaviour of DNA, the melting temperature  $T_m$  which is defined as the temperature where half of the total base pairs get non-bonded was studied. Intercalation of synthesized organics and metallointercalators generally results in considerable increase in melting temperature ( $T_m$ ). Thermal denaturation experiments were carried out by monitoring the absorption of CT DNA in 50  $\mu$ M concentration for the nucleotides at 260 nm with different temperature in the presence (10  $\mu$ M complex) and the absence of each complex. The melting temperature ( $T_m$ , the temperature at which 50% of double stranded DNA becomes single stranded) and the curve width ( $\sigma T$ , the temperature range between which 20 and 80% of the absorption increases occurred) were recorded.

### 2.6. Antioxidant Assay

#### 2.6.1. Superoxide Dismutase Activity (SOD)

The superoxide dismutase activity (SOD) of the copper complexes were evaluated using alkaline DMSO as source of superoxide radicals ( $O_2^{\cdot -}$ ) generating system in association with nitro blue tetrazolium chloride (NBT) as a scavenger of superoxide. Add 2.1 mL of 0.2 M potassium phosphate buffer (pH 8.6) and 1 mL of 56  $\mu$ L of NBT solutions to the different concentration of copper complex solution. The mixtures were kept in ice for 15 min and then 1.5 mL of alkaline DMSO solution was added while stirring. The absorbance was monitored at 540 nm against

a sample prepared under similar condition except NaOH was absent in DMSO.

### 2.7. Hydrogen Peroxide Assay

A solution of hydrogen peroxide (2.0 mM) was prepared in phosphate buffer (0.2 M, 7.4 pH) and its concentration was determined spectrophotometrically from absorption at 230 nm. The complexes of different concentration and vitamin C (100  $\mu$ g/mL) were added to 3.4 mL of phosphate buffer together with hydrogen peroxide solution (0.6 mL). An identical reaction mixture without the sample was taken as negative control. The absorbance of hydrogen peroxide at 230 nm was determined after 10 min against the blank (phosphate buffer).

#### 2.7.1. Catalase Activity

CAT activity in erythrocytes was determined according to spectrophotometric procedure by Beers and Sizer [23] and expressed in Bergmeyer units (BU/g Hb). CAT activity was measured at 25 °C by recording  $H_2O_2$  decomposition at 240 nm. One BU of CAT activity is defined as the amount of enzyme decomposing 1 g of  $H_2O_2$ /min.

#### 2.7.2. Antimicrobial Activities

The antibacterial activity of samples was determined using a well diffusion method. The antibacterial activities were performed by using *Staphylococcus aureus*, *Escherichia coli*, *Klebsiella pneumoniae*, *Proteus vulgaris* and *Pseudomonas aeruginosa*, respectively.

The nutrient agar medium was boiled to dissolve completely and sterilized at 15 lbs pressure (120 °C). After sterilization, 20 mL of media was poured into the sterilized petri plates. These plates were kept at room temperature and the medium got solidified in the plates. Then, it was inoculated with microorganisms using sterile swabs. The stock solutions were prepared by dissolving the compounds in appropriate solvents. The sample solutions were filled in the incubated plates using a micropipette and incubated for 24 h at 37 °C. During incubation period, the sample solution was diffused into the gel and inhibited the growth of the microorganism. The zone of inhibition was developed on the plate and measured.

## 3. Results and Discussions

The metal complexes are soluble in  $CHCl_3$ , DMSO, DMF and insoluble in water. The elemental analysis data of the Schiff bases and their metal complexes are equivalent with the calculated results from the empirical formula of each compound (Table 1). The Cu(II) complexes were dissolved in DMSO and the molar conductivities of  $10^{-3}$  M of their solution at room temperature were measured. The lower molar conductivity values of copper complexes were found in the range of (2–6)  $ohm^{-1} cm mol^{-1}$  suggesting them to be non-electrolytes which is evidenced the presence of acetate ions in coordination sphere. The analytical data are in a good agreement with the proposed stoichiometry  $[CuL(OAc)_2]$  of all the complexes. Furthermore, the magnetic moment measurements were recorded at room temperature lie in between 1.74 and 1.79 B.M. corresponding to the presence of one unpaired electron and it supports the square planar geometry around central copper ion.

### 3.1. NMR Spectral Features

The  $^1H$  NMR spectra of ligands were recorded in DMSO solution at room temperature. All the protons were found to be in their expected region. The ligand  $L^2$  showed the following spectral features for Knoevenagel condensate of acetoacetaanilide moiety: the peak arises at 6.5–8.4 ppm (m, 5H) corresponds to aromatic protons of acetoacetanilide ring, phenyl multiplet of salicylaldehyde was observed at 7.2–7.6 (m, 4H), methyl protons at 2.1 ppm (s, 3H), and –OH at 10.2 (s, H), respectively. In addition, peak appeared at 7.3 ppm, which is

**Table 1**

Physical characterization, analytical, molar conductance and magnetic susceptibility data of the ligands and their complexes.

Compound	Yield (%)	Color	(Found) calc				(ohm <sup>-1</sup> cm mol <sup>-1</sup> )	$\mu_{\text{eff}}$ (BM)
			Cu	C	H	N		
L <sup>1</sup>	67	Pale brown	–	68.68 (68.62)	4.51 (4.56)	12.52 (12.50)	–	–
L <sup>2</sup>	76	Dark yellow	–	68.24 (68.21)	4.25 (4.29)	12.84 (12.89)	–	–
L <sup>3</sup>	68	Brown	–	61.18 (61.24)	3.65 (3.59)	13.14 (13.21)	–	–
L <sup>4</sup>	74	Dark brown	–	67.10 (67.15)	4.78 (4.72)	11.86 (11.92)	–	–
[CuL <sup>1</sup> (OAc) <sub>2</sub> ]	56	Reddish brown	9.16 (9.21)	55.36 (55.28)	3.63 (3.78)	10.22 (10.19)	3	1.74
[CuL <sup>2</sup> (OAc) <sub>2</sub> ]	78	Yellowish brown	9.35 (9.28)	54.74 (54.77)	3.41 (3.48)	10.33 (10.31)	6	1.79
[CuL <sup>3</sup> (OAc) <sub>2</sub> ]	72	Black	8.05 (8.18)	53.19 (53.13)	3.57 (3.53)	8.87 (8.72)	4	1.77
[CuL <sup>4</sup> (OAc) <sub>2</sub> ]	59	Black	8.23 (8.27)	57.53 (57.48)	4.44 (4.48)	9.07 (9.14)	2	1.76

assigned to free –NH group of acetoacetanilide moiety. Moreover, the multiplets within the range 7.8–8.2 ppm (m, 8H) were assigned to the aromatic protons of benzothiazole ring [24]. It was concluded that the absence of amino group of 2-aminobenzothiazole indicated the formation of Schiff base ligand system.

### 3.2. FT-IR

The characteristic IR bands for the synthesized ligands and copper complexes were listed in the given Table 2. The ligand L<sup>2</sup> exhibits two IR bands assigned to imine  $\nu(\text{C}=\text{N})$  groups of 2-aminobenzothiazoles moiety at 1647 cm<sup>-1</sup> and 1622 cm<sup>-1</sup> are shifted to a lower frequency of 1626 cm<sup>-1</sup> and 1608 cm<sup>-1</sup> after complexation [25]. Also, the new IR bands near at 435 cm<sup>-1</sup> and 505 cm<sup>-1</sup> were assigned to (M–N) and  $\nu(\text{M–O})$  [26]. In addition the appearance of new bands at 1368 cm<sup>-1</sup> and 1270 cm<sup>-1</sup> corresponds to symmetric and asymmetric stretching for  $\nu(\text{M–O})$ . It is also further supported by the appearance of bands between 1370 cm<sup>-1</sup>–1374 cm<sup>-1</sup> and 1268–1274 cm<sup>-1</sup> attributed to  $\nu_{\text{asym}}(\text{COO}^-)$  and  $\nu_{\text{sym}}(\text{COO}^-)$  respectively for two copper complexes. The difference in  $\Delta\nu$  between  $\nu_{\text{asym}}(\text{COO}^-)$  and  $\nu_{\text{sym}}(\text{COO}^-)$  in metal complexes was ~100 cm<sup>-1</sup> suggests the mode of coordination of carboxylate group (i.e., acetate ion) in copper complexes in a monodentate manner. It was reported that the copper complexes were behaved as bidentate and coordinate through azomethine nitrogen atoms. The IR Spectral features were reinforced the conclusion drawn from conductance measurements [27].

### 3.3. Electronic Spectral Features

The electronic absorption spectra of the Schiff base ligands and their copper complexes in DMSO solvent were recorded at room temperature. The band positions of the absorption maxima; band assignments and the proposed geometry mentioned in Table 3. The absorption spectrum for ligand L<sup>1</sup> showed a band at 270 nm attributed to  $n-\pi^*$

transitions within the Schiff base molecule. The electronic spectrum of the corresponding complex [CuL<sup>1</sup>(OAc)<sub>2</sub>] in DMSO reveals a broad band at 427 nm assigned to  $^2\text{B}_{1g} \rightarrow ^2\text{A}_{1g}$  transition which is characteristic of square planar environment around the copper(II) ion. Similar spectral features were observed for other copper complexes [28].

### 3.4. DNA Binding Experiments

#### 3.4.1. Cyclic Voltammetric Studies

Cyclic voltmetric technique is the versatile technique useful for the DNA binding ability of electro active species. In the absence of DNA, Cyclic voltammogram of [CuL<sup>1</sup>(OAc)<sub>2</sub>] exhibited cathodic and anodic peaks were observed at –0.241 V and –0.080 V which are assigned to Cu(II)/Cu(I) conversion. Cyclic voltammogram of [CuL<sup>2</sup>(OAc)<sub>2</sub>] showed two segments of cathodic and anodic peaks. The first segment, cathodic and anodic peaks were observed at 0.120 V and 0.231 V, respectively. This showed oxidation from +1 to +2 form at a cathodic peak potential. This showed unusual oxidation state of ligand system. This showed reduction occurs from +2 to +1 form at a cathodic peak potential.

When addition of various concentration of CT-DNA in the same concentration of complex indicated decreases voltmetric peak current which is shown in the Fig. 1 & Fig. 2 for [CuL<sup>1</sup>(OAc)<sub>2</sub>] & [CuL<sup>2</sup>(OAc)<sub>2</sub>]. This is highly due to diffusion of the equilibrium mixture of free and DNA-bound metal complex to the electrode surface, in which the peak potentials both  $E_{\text{pa}}$  and  $E_{\text{pc}}$  as well as  $E_{1/2}$  have a shift to negative potential. The observed separation of cathodic and anodic potentials,  $\Delta E_p = -0.215$  and  $-0.250$  for [CuL<sup>1</sup>(OAc)<sub>2</sub>] & [CuL<sup>2</sup>(OAc)<sub>2</sub>] indicated that the reaction of copper complexes on the working electrode was quasi reversible redox process.

The peak currents observed for all copper complexes showed changes in current indicated that both metal complex interact with CT-DNA through partial intercalative mode [29]. It was reported that higher

**Table 2**Characteristic IR bands of the Schiff base ligands and its copper complexes (in cm<sup>-1</sup>).

Compound	$\nu(\text{C}=\text{N})$	$\nu(\text{C}=\text{N})$	$\nu(\text{M–O})$	$\nu(\text{M–N})$	$\nu_{\text{asym}}(\text{COO}^-)$	$\nu_{\text{sym}}(\text{COO}^-)$
L <sup>1</sup>	1628	1642	–	–	–	–
L <sup>2</sup>	1622	1647	–	–	–	–
L <sup>3</sup>	1632	1641	–	–	–	–
L <sup>4</sup>	1627	1643	–	–	–	–
[CuL <sup>1</sup> (OAc) <sub>2</sub> ]	1610	1628	512	442	1374	1272
[CuL <sup>2</sup> (OAc) <sub>2</sub> ]	1608	1624	505	435	1368	1270
[CuL <sup>3</sup> (OAc) <sub>2</sub> ]	1603	1621	514	447	1370	1268
[CuL <sup>4</sup> (OAc) <sub>2</sub> ]	1607	1627	509	444	1371	1274

**Table 3**

Electronic spectra of Schiff base ligands and their copper complexes (nm).

Compound	Wavelength (nm)	Band assignments	Geometry	$K_b$ (M <sup>-1</sup> )	$\Delta G$ (cal)
L <sup>1</sup>	270	$\pi-\pi^*$	–	–	–
L <sup>2</sup>	285	$\pi-\pi^*$	–	–	–
L <sup>3</sup>	309	$n-\pi^*$	–	–	–
L <sup>4</sup>	319	$n-\pi^*$	–	–	–
[CuL <sup>1</sup> (OAc) <sub>2</sub> ]	437	$^2\text{B}_{1g} \rightarrow ^2\text{A}_{1g}$	Square planar	$3.23 \times 10^5$	–31,452
[CuL <sup>2</sup> (OAc) <sub>2</sub> ]	464	$^2\text{B}_{1g} \rightarrow ^2\text{A}_{1g}$	Square planar	$3.18 \times 10^5$	–30,527
[CuL <sup>3</sup> (OAc) <sub>2</sub> ]	467	$^2\text{B}_{1g} \rightarrow ^2\text{A}_{1g}$	Square planar	$3.27 \times 10^5$	–31,381
[CuL <sup>4</sup> (OAc) <sub>2</sub> ]	439	$^2\text{B}_{1g} \rightarrow ^2\text{A}_{1g}$	Square planar	$3.24 \times 10^5$	–31,309



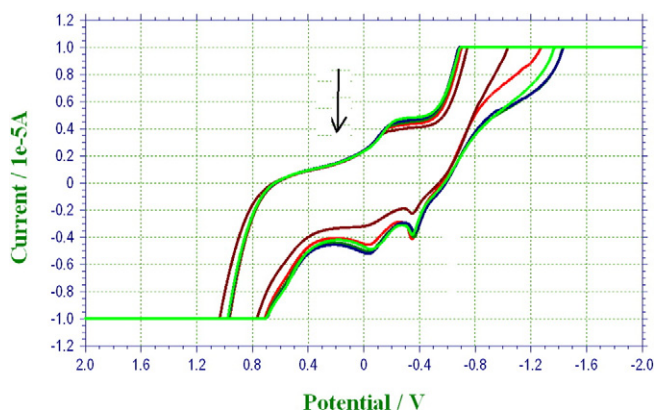


Fig. 1. Cyclic voltammogram of  $[\text{CuL}^1(\text{OAc})_2]$  in the presence and absence of DNA.

decrease of current observed for the complex  $[\text{CuL}^1(\text{OAc})_2]$  had stronger binding affinity with CT-DNA and indicated all other copper complexes were bind *via* partial intercalative binding mode [30] and their electrochemical parameters are given in Table 4.

### 3.4.2. Absorption Spectral Titrations

In the DNA binding studies, Hyper and hypochromic effects are two important spectral features concerns about the influence of molecules with DNA either expansion or contraction of DNA structure. In general, hypochromism was observed in the spectrum indicates the molecule binding with DNA through intercalation mode. The extent of hypochromism corresponds to the strength of intercalative binding interactions. The ansence of any isobestic points in the spectrum indicates more than one type of DNA-molecule interactions was observed. The metal ion, charge of chelate and nature of ligand surrounded on the metal center decides the nature binding with DNA. The DNA possesses many hydrogen bonding sites which are available both in the minor and major grooves and leads to groove binding of molecules.

The binding properties of complexes to the CT-DNA helix have been determined by electronic absorption spectral methods. The magnitude of hypochromism and red shift depends upon the strength of interaction between metal complexes and CT-DNA. As the DNA concentration is increased, the following changes to be observed in the absorbance and shift in wavelength of ligand as well as metal complexes. On the addition of CT-DNA, the copper complex of  $[\text{CuL}^1(\text{OAc})_2]$  showed broad peak at 437 nm which shoulder at 270 nm results in decrease in molar absorptivity (hypsochromism) blue shift of 2–7 nm shown in the Fig. 3. These data suggested that metal complex clearly bind to partial intercalative binding mode. The same binding features were observed for the  $[\text{CuL}^3(\text{OAc})_2]$  and  $[\text{CuL}^4(\text{OAc})_2]$  complexes.

On the addition of CT-DNA, The  $[\text{CuL}^2(\text{OAc})_2]$  complex showed broad peak at 464 nm which shoulder at 285 nm which results in

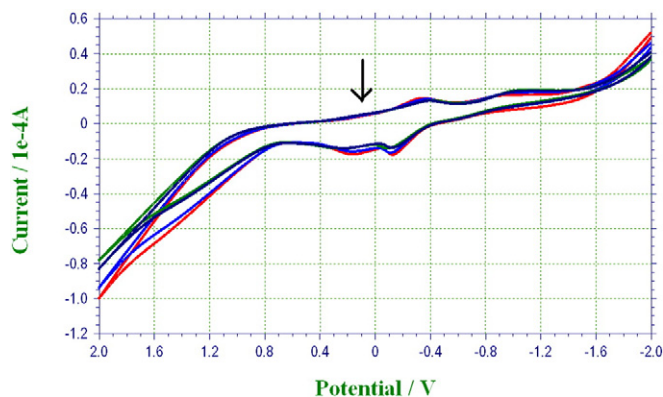


Fig. 2. Cyclic voltammogram of  $[\text{CuL}^2(\text{OAc})_2]$  in the presence and absence of DNA.

Table 4

Electrochemical parameters for the interaction of DNA with copper complexes.

Compound	Redox couple	$E_{1/2}$ (V)		$\Delta E_p$ (V)		$i_{pa}/i_{pc}$
		Free	Bound	Free	Bound	
$[\text{CuL}^1(\text{OAc})_2]$	$\text{Cu(II)} \rightarrow \text{Cu(I)}$	−0.160	−0.517	−0.321	−0.215	1.02
$[\text{CuL}^2(\text{OAc})_2]$	$\text{Cu(I)} \rightarrow \text{Cu(II)}$	−0.175	−1.475	−0.351	−0.250	1.18
$[\text{CuL}^3(\text{OAc})_2]$	$\text{Cu(II)} \rightarrow \text{Cu(I)}$	−0.265	−0.421	−0.142	−0.268	1.15
$[\text{CuL}^4(\text{OAc})_2]$	$\text{Cu(II)} \rightarrow \text{Cu(I)}$	−1.312	−1.562	−0.144	−0.210	1.12

increase in molar absorptivity (hypochromism) with hypochromic (blue) shift by 2–3 nm [31] indicating intercalative mode of binding seen between aromatic chromophore of metal complexes with CT-DNA in Fig. 4. The d-d transition for complexes at 464 nm indicates that the copper complexes interacts with  $\text{N}^7$  of guanine of CT-DNA. All these data were then fitted to Eq. (1) to obtain the intrinsic binding constant ( $K_b$ ) values and resulted that  $[\text{CuL}^1(\text{OAc})_2]$  complexes bind with DNA by partial intercalation mode [32–34]. The Intrinsic binding constants ( $K_b$ ) for copper complexes were in the range of  $3.18 \times 10^5 \text{ M}^{-1}$ – $3.27 \times 10^5 \text{ M}^{-1}$  are less when compared with the reported few intercalating complexes  $[\text{Ru}(\text{bpy})_2(\text{dppz})]^{2+}$  ( $4.90 \times 10^6 \text{ M}^{-1}$ ) [33] and  $[\text{Ru}(\text{bpy})_2(\text{HBT})]^{2+}$  ( $5.71 \times 10^6 \text{ M}^{-1}$ ). Binding energy is the measure of stability of complexes. The binding energy between DNA base pairs and complexes were calculated according to the equation  $\Delta G = -RT \ln K_b$  and the values are tabulated in the Table 3.

### 3.4.3. Thermal Denaturation

The thermal behaviour of CT-DNA in the presence of complexes gave insight into their conformational changes when temperature is raised when temperature is raised and information about the interaction strength of the complexes with DNA. The double-stranded DNA tends to gradually dissociate to single strands on increase in the solution temperature and generates a hyperchromic effect on the absorption spectra of DNA bases (at 316 nm). In the present study melting temperature ( $T_m$ ) of DNA in the absence of copper complexes was found to be  $54 \pm 1^\circ \text{C}$ . Under the same set of experimental conditions, addition of complexes increased the melting temperature  $T_m$  ( $\pm 1^\circ \text{C}$ ) from  $10^\circ \text{C}$  to  $15.3^\circ \text{C}$ , for all copper complexes respectively. This experimental data indicates that the all  $\text{Cu(II)}$  complexes of peptides has interaction with double helix CT-DNA. The intercalation of small molecules into the double helix has as a result an increase of melting temperature at which the double helix denaturates into single helix DNA, The significant increase of  $T_m$  ( $\Delta T_m = 15.3^\circ \text{C}$ ) suggests that the interaction of the all copper complexes with DNA is performed through partial intercalation shown in the Fig. 5 [35,36].

### 3.4.4. Antioxidant Activity

In this study radical scavenging properties of copper complexes were determined by the NBT assay method and hydrogen peroxide assay [37,38]. The generation of Superoxide radicals is determined by

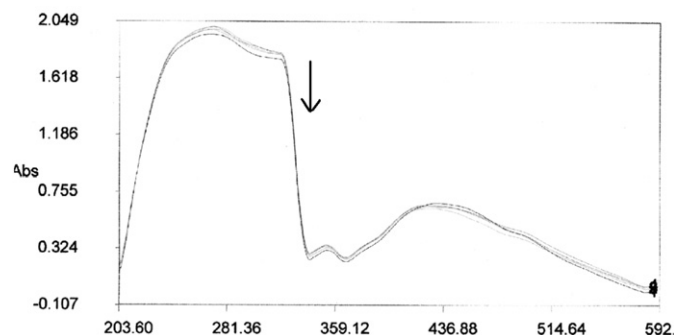


Fig. 3. Electronic spectra of  $[\text{CuL}^1(\text{OAc})_2]$  in the presence and absence of DNA.

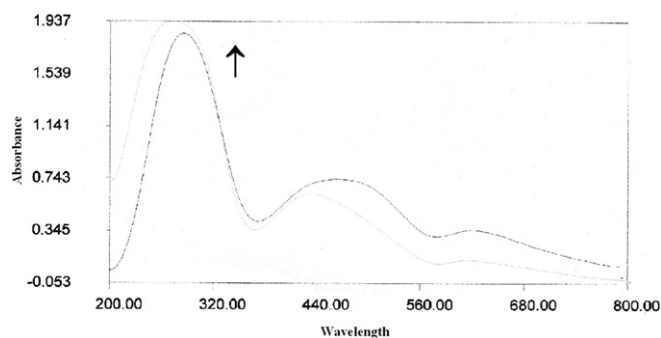


Fig. 4. Electronic spectra of  $[\text{CuL}^2(\text{OAc})_2]$  in the presence and absence of DNA.

the percentage of inhibition of the reduction of NBT ( $\text{IC}_{50}$ ). The significant  $\text{IC}_{50}$  values are determined by UV–Vis. Spectroscopy. It has been revealed that the synthesized copper complexes exhibited a quite strong antioxidant activity in the range of 30–47  $\mu\text{mol dm}^{-3}$ . The reactivity of free radicals can be neutralized by the donation of electron or hydrogen, from the above fact it has been suggested that the presence of hydroxy ligand system of  $[\text{CuL}^2(\text{OAc})_2]$  act as the efficient hydrogen donors to stabilize the unpaired electrons and scavenging free radicals. Further it was supported by the fact, lower the  $\text{IC}_{50}$  values higher ability of donating hydrogen. So scavenging activity of  $[\text{CuL}^2(\text{OAc})_2]$  copper complex is in the order of  $[\text{CuL}^2(\text{OAc})_2] > [\text{CuL}^3(\text{OAc})_2] > [\text{CuL}^1(\text{OAc})_2] > [\text{CuL}^4(\text{OAc})_2]$  which are graphically represented in the Figs. 6 & 7 and the values are tabulated in the Table 5. Curcumin prevents the oxidation of hemoglobin and inhibits lipid peroxidation. The antioxidant activity of curcumin could be mediated through antioxidant enzymes such as superoxide dismutase, catalase, and glutathione peroxidase [39]. Curcumin acts as a superoxide radical scavenger report describes the H-atom donation from the  $\beta$ -diketone moiety to a lipid alkyl or a lipid peroxy radical as a potentially more important antioxidant action of curcumin [40]. So the curcumin analog system of present system also posses higher antioxidant activity.

Cu(II) complexes containing small bioligands are considered as efficient therapeutic agents because they mimic SOD activity [41,42]. In these Cu(II) complexes, Cu-center is involved in a redox cyclic process by successive encounters with superoxide and producing and  $\text{H}_2\text{O}_2$  at the reactive site and can easily dismutate the excess of intracellular  $\text{O}_2^-$  and  $\text{H}_2\text{O}_2$  and increasing the concentration which is act as excellent SOD mimetics due to its effective bioligand system of 2-aminobenzothiazole.

The redox property of copper complexes plays a key role in radical neutralization and disproportionation of toxic species into nontoxic species. All the synthesized copper complexes showed redox behaviour ( $\text{Cu}^{2+}/\text{Cu}^+$ ) of negative potentials. It indicates that copper complexes act as good antioxidant systems. The unusual oxidation state was

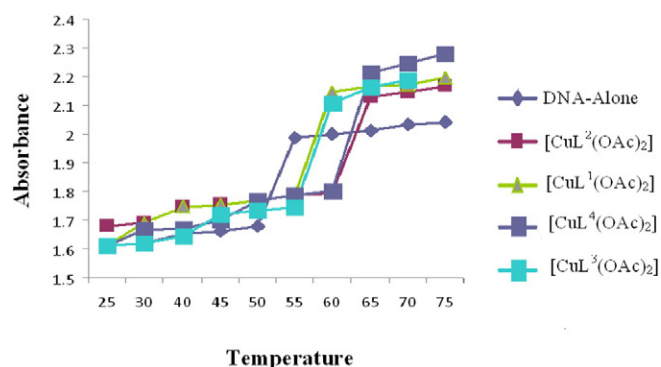


Fig. 5. Thermal Denaturation Curve for all Cu(II) complexes.

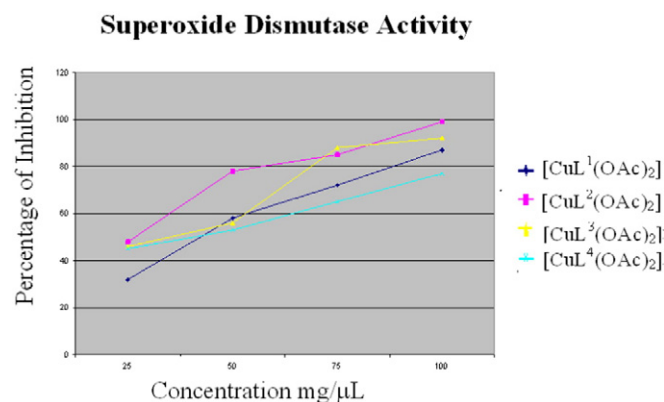


Fig. 6. Hydrogen peroxide activity of Cu(II) complexes in ( $\mu\text{mol dm}^{-3}$ ).

stabilized by the proposed ligand systems. It is also disproportionate  $\text{H}_2\text{O}_2$  by converting it into the  $\text{H}_2\text{O}$  and  $\text{O}_2$ .

In Alzheimer's disease, the metal contamination may produce oxidative stress and protein aggregation into A $\beta$ -peptides. In general, antioxidant and enzyme mimetic compounds may act as good therapeutic candidates for Alzheimer's disease for reduction of ROS levels and peptide cleavage. In the present study, all the copper complexes showed enzyme mimetic activities. The prepared copper complexes act as good candidates for antialzheimer's agents.

### 3.4.5. Antimicrobial Activity

The *in vitro* antimicrobial activities of the investigated compounds were tested against the five bacterial species, *Staphylococcus aureus*, *Escherichia coli*, *Klebsiella pneumoniae*, *Proteus vulgaris*, and *Pseudomonas aeruginosa* by disc diffusion method [43]. The MIC values of all the compounds against the microorganism are summarized in the Table 6.

The comparative study (MIC) of ligands with their copper complexes indicated that the complexes have higher activities than the synthesized ligands. In general, the synthesized metal complexes have higher biological activities compared to the free ligands. The increased inhibition activity of the metal complexes can be explained on the basis of Tweedy's chelation theory [44]. In metal complexes, on chelation the polarity of the metal ion will be reduced to a greater extent due to the overlap of the ligand orbital and partial sharing of the positive charge of the metal ion with donor groups. Further, it increases the delocalization of  $\pi$ -electrons over the whole chelate ring.

### 3.4.6. Highly Conjugated System

The enhanced activity of the complexes may also be explained on the basis of conjugation. Copper complexes have higher activity than ligands due to the presence of highly conjugated curcumin analog system. Since The whole ligand system could act as highly conjugated

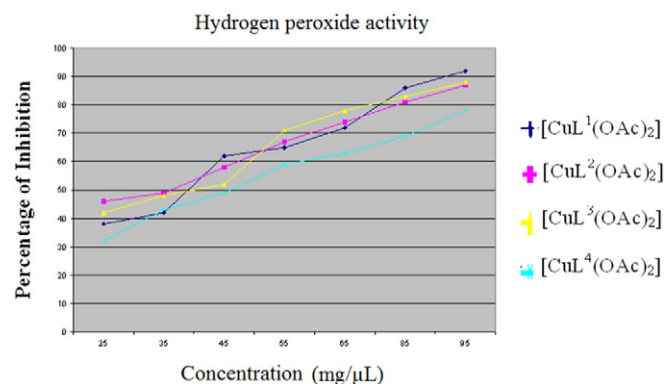
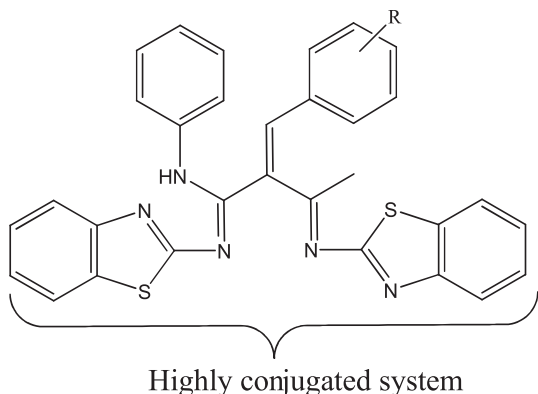


Fig. 7. Superoxide dismutase activity of Cu(II) complexes in ( $\mu\text{mol dm}^{-3}$ ).

**Table 5**  
Antioxidant activity of Schiff base copper complexes in ( $\mu\text{mol dm}^{-3}$ ).

Compound	IC <sub>50</sub> ( $\mu\text{mol dm}^{-3}$ ) H <sub>2</sub> O <sub>2</sub>	IC <sub>50</sub> ( $\mu\text{mol dm}^{-3}$ ) O <sub>2</sub> <sup>•−</sup>
[CuL <sup>1</sup> (OAc) <sub>2</sub> ]	40	40
[CuL <sup>2</sup> (OAc) <sub>2</sub> ]	36	30
[CuL <sup>3</sup> (OAc) <sub>2</sub> ]	38	37
[CuL <sup>4</sup> (OAc) <sub>2</sub> ]	47	46
Vitamin C	0.02	0.05

system may also responsible for higher antimicrobial activities. In the present ligand system, the Knoevengel condensate of  $\beta$ -ketoanilide has active carbonyl group that makes high liphophilic behaviour. It enhances the pharmacological efficiencies when coordinating with copper ion.



### 3.4.7. Effect of Substitute

Further, inhibitory action gets enhanced with the introduction of electron-withdrawing substitute in the phenyl ring than electron-releasing substitute. The increase in antibacterial activity is due to faster diffusion of the free ligands with electron withdrawing groups and metal complexes as a whole through the cell membrane or due to the combined activity effect of ligand and metal. Such increased activity of the metal chelates can be explained as polarity of the metal ion will be reduced to a greater extent due to the overlap of the ligand orbital and partial sharing of the positive charge of the metal ion with electron releasing groups.

The complexes with electron releasing substitutes such methoxy group of copper complexes showed increased activity than the hydroxyl group of copper complex due to comparatively faster diffusion of copper complex into cell membrane in the presence of methoxy group [45]. The antimicrobial activity of synthesized copper complexes in the order of [CuL<sup>3</sup>(OAc)<sub>2</sub>] > [CuL<sup>4</sup>(OAc)<sub>2</sub>] > [CuL<sup>1</sup>(OAc)<sub>2</sub>] > [CuL<sup>2</sup>(OAc)<sub>2</sub>] and their (MIC) values are tabulated in the Table 6. Furthermore, the formation of hydrogen bond through imine group with the active center of cell

**Table 6**  
Minimum inhibitory concentration values of the synthesized compounds against the growth of four bacteria (in  $\mu\text{g/mL}$ ).

Compound	<i>Staphylococcus aureus</i>	<i>Escherichia coli</i>	<i>Klebsiella pneumoniae</i>	<i>Pseudomonas aeruginosa</i>	<i>Proteus vulgaris</i>
L <sup>1</sup>	28	26	32	27	30
L <sup>2</sup>	31	29	36	31	33
L <sup>3</sup>	22	21	27	25	24
L <sup>4</sup>	24	25	26	22	29
[CuL <sup>1</sup> (OAc) <sub>2</sub> ]	13	12	11	14	12
[CuL <sup>2</sup> (OAc) <sub>2</sub> ]	12	11	13	12	0.11
[CuL <sup>3</sup> (OAc) <sub>2</sub> ]	9	6	8	7	8
[CuL <sup>4</sup> (OAc) <sub>2</sub> ]	11	8	9	9	10
Streptomycin	2	1.8	2.5	1.9	1.8

constitutions, resulting in interfering with the normal cell process possessing superior the pharmacological efficiencies when coordinating with copper ion.

### Acknowledgement

We express our sincere thanks to the Chancellor, Noorul Islam Centre for Higher Education, Kumaracoil for providing research facilities. This work was financially supported by DST, New Delhi under Young scientist scheme 002/2014.

### References

- [1] Y. Kiso, Y. Suzuki, N. Watanabe, Y. Oshima, H. Hikino, Med. Res. 49 (3) (1983) 185.
- [2] N. Vekatesan, Br J Pharmacol 40 (3) (1998) 413.
- [3] R. Srivastava, M. Diskshit, R.C. Srimal, B.N. Dhawan, Thromb Res 40 (3) (1985) 413.
- [4] M. Diskshit, L. Rastogi, R.S. Shukla, R.C. Srimal, Indian J Med Res 101 (1995) 31.
- [5] Subash Padhye, Huanjie Yang, Abeda Jamadar, Quizhi Cindi Cui, Deepak Chavan, Kristin Dominiak, Jaclyn McKinney, Sanjeev Banerjee, Q. Ping Dou, Fazul H. Sarkar, Pharm Res (2009) 415.
- [6] R.D. Jones, D.A. Summerville, F. Basolo, Chem Rev 79 (1979) 139.
- [7] G.H. Olie, S. Olive, Springer, Berlin, 1984, 152.
- [8] H. Dugas, C. Penney, Springer, New York, 1981, 435.
- [9] J.D. Margerum, L.J. Miller, Wiley Interscience, New York, 1971, 569.
- [10] P.A. Vigato, S. Tamburini, Coord Chem Rev 248 (2004) 1717.
- [11] J.A. Obaleye, C.A. Akinremi, E.A. Balogun, J.O. Adebayo, African J Boitechnology 24 (2007) 2826.
- [12] A.A. Osowole, S.A. Balogun, European J Appl Sciences (2012) 6.
- [13] I. Sakyan, E. Logoglu, S. Arslan, N. Sari, N. Sakiyar, Biol Met 17 (2004) 115.
- [14] R.C. Sharma, V.K. Varshney, J Inorg Biochem 41 (1999) 299.
- [15] P. Vicini, A. Geronikaki, M. Incerti, B. Busonera, G. Poni, C.A. Cabrasc, P.L. Collac, Bioorg Med Chem 11 (2003) 4785.
- [16] A. Hitoushi, F. Hideyumi, M. Manaby, Tokayorkiv. Polyhedron 16 (1997) 3787.
- [17] K. Krishnankutty, M.B. Ummathur, D.K. Babu, J. Serbian, Chem Soc 75 (2010) 639.
- [18] N. Raman, S.J. Raja, J. Joseph, J.D. Raja, Russ J Coord Chem 33 (2007) 3.
- [19] P.U. Maheshwari, M. Palaniandavar, Inorg Chim Acta 357 (2004) 901.
- [20] H. Sigel (Ed.), Marcel Dekker, New York, 1981.
- [21] R. Pradhan, A.M. Thomas, A. Mukherjee, S. Dhar, M. Nethaji, A.R. Chakravarty, Indian J Chem A 44 (2005) 18.
- [22] I. Fridovich, Annu Rev Biochem 64 (1995) 97.
- [23] R. Beers, T. Sizer, J Biol Chem 195 (1952) 133–140.
- [24] Robert M. Silverstein, S.X. Francis, Webster, Spectroscopic Identification of Organic Compounds, sixth ed. Wiley India, (2009) 165.
- [25] M.A. Neelakantan, M. Esakkiammal, S.S. Marriappan, J. Dharmaraja, T. Jeyakumar, Indian J Pharm Sci 72 (2010) 216.
- [26] N. Raman, V. Mutijuraj, S. Rovichandran, Kulandaisamy, Ind Acad Sci 115 (5) (2003) 161.
- [27] N. Raman, S. Sobha, M. Selvaganapathy, R. Mahalakshmi, Spectrochim. Acta A Mol. Biomol. Spectrosc. 96 (2012) 698.
- [28] P.K. Ray, B. Kauffman, Inorg Chim Acta 173 (1990) 207.
- [29] Pathan H. Aishakhanam, Bakale P. Raghavendra, Naik N. Ganesh, Frampton S. Christopher, Gudasi B. Kalagouda, Polyhedron vol. 34 (2012) 149.
- [30] N. Raman, A. Selvan, P. Manissankar, Spectrochim Acta A 76 (2010) 161.
- [31] Chellaian Justin Dhanaraj, Jijo Johnson, J Photochem Photobiol B Biol 161 (2016) 108–121.
- [32] Balaraman Selvakumar, Venugopal Rajendiran, Palanisamy Uma Maheswari, Helen Stoeckli-Evans, Mallayan Palaniandavar, J Inorg Chem 100 (2006) 316.
- [33] S.R. Smith, G.A. Neyhart, W.A. Karlsbeck, H.H. Thorp, New J Chem 18 (1994) 397.
- [34] Mehvash Zaki, Mohd. Afzal, Musheer Ahmad, Sartaj Tabassum, J Photochem Photobiol B Biol 161 (2016) 318–327.
- [35] C.N. Sudhamani, H.S. Bhojya Naik, D. Girija, T. Aravinda, International Research Journal of Pure & Applied Chemistry 1 (2) (2011) 42.
- [36] Ng. Lingthoingambi, N. Rajen Singh, M. Damayanti, J Chem Pharm Res 3 (6) (2011) 187–194.
- [37] L.M. Gaetke, C.K. Chow, Toxicology 189 (2003) 147.
- [38] R.J. Ruch, S.J. Chenge, J.E. Klaunig, Carcinogenesis 10 (1989) 1003.
- [39] B.B. Aggarwal, A. Kumar, A.C. Bharti, Anticancer potential, Anticancer Res 23 (2003) 363.
- [40] M. Nabiuni, Z. Nazari, S. Abdolhamid Angaji, Z. Safayi Nejad, Aust J Basic Appl Sci 5 (2011) 2224–2240.
- [41] P.P. Deschamps, P. Kulkarani, B. Sarkar, Inorg Chem 43 (2004) 3338.
- [42] H. Ohtsu, Y. Shimazaki, A. Odani, O. Yamauchi, W. Mori, S. Itoh, S. Fukuzumi, J. Am. Chem. 13 (2000) 5733.
- [43] A.W. Bauer, W.M. Kirby, J.C. Sherris, M. Turck, Am J Clin Pathol 45 (1966) 493.
- [44] B.G. Tweedy, Phytopathology 55 (1964) 910.
- [45] N. Raman, J. Joseph, Russ J Inorg Chem 55 (2010) 1064.